In-vivo evaluation of neuronal and glial changes in amyotrophic lateral sclerosis with diffusion tensor spectroscopy

Author(s):
Reischauer, Carolin; Gutzeit, Andreas; Neuwirth, Christoph; Fuchs, Alexander; Sartoretti-Schefer, Sabine; Weber, Markus; Czell, David

Publication date:
2018

Permanent link:
https://doi.org/10.3929/ethz-b-000309040

Originally published in:
NeuroImage: Clinical 20, https://doi.org/10.1016/j.nicl.2018.10.001

NeuroImage: Clinical 20 (2018) 993–1000

Contents lists available at ScienceDirect

NeuroImage: Clinical

journal homepage: www.elsevier.com/locate/ynicl

In-vivo evaluation of neuronal and glial changes in amyotrophic lateral sclerosis with diffusion tensor spectroscopy

Carolin Reischauer[a,b,*], Andreas Gutzeit[a,c,d], Christoph Neuwirth[e], Alexander Fuchs[b], Sabine Sartoretti-Schefer[f], Markus Weber[e], David Czell[g,h]

[a] Institute of Radiology and Nuclear Medicine, Clinical Research Unit, Hirslanden Hospital St. Anna, Lucerne, Switzerland
[b] Institute for Biomedical Engineering, ETH and University of Zurich, Zurich, Switzerland
[c] Department of Chemistry and Applied Biosciences, ETH Zurich, Zurich, Switzerland
[d] Department of Radiology, Paracelsus Medical University Salzburg, Salzburg, Austria
[e] Neuromoscular Disease Unit, ALS Clinic, Cantonal Hospital St. Gallen, St. Gallen, Switzerland
[f] Department of Radiology, Cantonal Hospital Winterthur, Winterthur, Switzerland
[g] Department of Neurology, Cantonal Hospital Winterthur, Winterthur, Switzerland
[h] Department of Neurology, Spital Linth, Uznach, Switzerland

ARTICLE INFO

Keywords:
Amyotrophic lateral sclerosis
Neurodegeneration
Diffusion-weighted spectroscopy
Tissue microstructure
Intracellular metabolites

ABSTRACT

Diffusion tensor spectroscopy (DTS) combines features of magnetic resonance spectroscopy and diffusion tensor imaging and permits evaluating cell-type specific properties of microstructure by probing the diffusion of intracellular metabolites. This exploratory study investigates for the first time microstructural changes in the neuronal and glial compartments of the brain of patients with amyotrophic lateral sclerosis (ALS) using DTS. To this end, the diffusion properties of the neuronal metabolite tNAA (*N*-acetylaspartate + *N*-acetylaspartylglutamate) and the predominantly glial metabolites tCr (creatine + phosphocreatine) and tCho (choline-containing compounds) were evaluated in the primary motor cortex of 24 ALS patients and 27 healthy controls. Significantly increased values in the diffusivities of all three metabolites were found in ALS patients relative to controls. Further analysis revealed more pronounced microstructural alterations in ALS patients with limb onset than with bulbar onset relative to controls. This observation may be related to the fact that the spectroscopic voxel was positioned in the part of the motor cortex where the motor functions of the limbs are represented. The higher diffusivities of tNAA may reflect neuronal damage and/or may be a consequence of mitochondrial dysfunction in ALS. Increased diffusivities of tCr and tCho are in line with reactive microglia and astrocytes surrounding degenerating motor neurons in the primary motor cortex of ALS patients. This pilot study demonstrates for the first time that cell-type specific microstructural alterations in the brain of ALS patients may be explored in vivo and non-invasively with DTS. In conjunction with other microstructural magnetic resonance imaging techniques, DTS may provide further insights into the pathogenic mechanisms that underlie neurodegeneration in ALS.

1. Introduction

Amyotrophic lateral sclerosis (ALS) is a neurologic disorder characterized by progressive degeneration of upper and lower motor neurons (Rowland and Shneider 2001). ALS is uniformly fatal but shows a markedly heterogeneous clinical presentation and course with a median survival time of 2–4 years from the onset of symptoms (Beghi et al. 2006).

Among various magnetic resonance (MR) techniques, spectroscopy has shown potential for assessing pathological abnormalities in ALS. The most commonly measured brain metabolites using proton MR spectroscopy are tNAA (*N*-acetylaspartate + *N*-acetylaspartylglutamate), which is almost exclusively localized within neurons/axons (Simmons et al. 1991) and is thus considered a neuronal marker, tCr (creatine + phosphocreatine), which is linked to cell energy metabolism, and tCho (soluble choline-containing compounds), which are related to cellular membrane turnover reflecting cellular proliferation. The latter two are predominantly found in glial cells (Brand et al. 1993; Le Belle et al. 2002; Urenjak et al. 1993). In ALS, spectroscopic studies, in particular of the primary motor cortex

* Corresponding author at: Hospital St. Anna, Clinical Research Unit, Institute of Radiology and Nuclear Medicine, St. Anna-Strasse 32, CH-6006 Lucerne, Switzerland.
E-mail address: carolin.reischauer@hirslanden.ch (C. Reischauer).

https://doi.org/10.1016/j.nicl.2018.10.001
Received 3 June 2018; Received in revised form 21 August 2018; Accepted 2 October 2018
Available online 03 October 2018

(PMC), have found significantly reduced concentrations of tNAA (Bowen et al. 2000; Bradley et al. 1999; Gredal et al. 1997; Pohl et al. 2001; Schuff et al. 2001) and significantly deceased tNAA/tCr (Block et al. 1998; Chan et al. 1999; Pioro et al. 1994; Pohl et al. 2001; Wang et al. 2006), tNAA/tCho (Block et al. 1998; Pohl et al. 2001; Wang et al. 2006), and tNAA/(tCho + tCr) ratios (Rooney et al. 1998; Suhy et al. 2002). These findings have been interpreted as evidence of neuronal loss in ALS. Furthermore, significantly reduced concentrations of tCr (Pohl et al. 2001), increased concentrations of tCho (Bowen et al. 2000), and elevated tCho/tCr ratios have been observed (Block et al. 1998; Pohl et al. 2001).

MR spectroscopy delivers cell-type specific information but it cannot provide structural information. In contrast, diffusion tensor imaging (DTI) (Basser et al. 1994a, 1994b) is sensitive to alterations in tissue microstructure but lacks pathologic specificity since water molecules reside in all tissue compartments. Diffusion tensor spectroscopy (DTS) (Basser et al. 1994b; Ellegood et al. 2006; Merboldt et al. 1993; Nicolay et al. 1995; Posse et al. 1993; Van Zijl et al. 1991) combines the compartment specificity of MR spectroscopy with the microstructural sensitivity of DTI and permits evaluating properties of cell-specific tissue microstructure by probing the diffusion of intracellular brain metabolites. In this manner, DTS allows inferring more specific information on the underlying tissue microstructure than DTI and thus features improved pathologic specificity. The methodology has been applied to several pathologies such as acute cerebral ischemia (Harada et al. 2002; Zheng et al. 2012), tumors (Colvin et al. 2008; Harada et al. 2002), mitochondrial cytopathies (Liu et al. 2011), multiple sclerosis (Bodini et al. 2018; Wood et al. 2012), systemic lupus erythematosus (Ercan et al. 2016), and migraine (Zielman et al. 2017).

This exploratory study investigates for the first time microstructural alterations in neurons and glial cells in the brain of ALS patients with DTS. To this end, the diffusion properties of the neuronal metabolite tNAA and the predominantly glial metabolites tCr and tCho are compared in the primary motor cortex of 24 ALS patients and 27 healthy controls. Changes in the parameters over time are explored and Spearman's rank correlations across times are calculated to delineate the relationship between clinical parameters and diffusion measures. Coefficients of variation (CVs) and inter-subject variabilities (ISVs) are assessed in the control group. For further exploratory analysis, the patient group is subdivided into limb-onset and bulbar-onset ALS patients and group comparisons are performed.

2. Materials and methods

2.1. Patients and control subjects

This prospective single-center study was approved by the local Ethics Committee (St. Gallen, Switzerland) and informed written consent was obtained from all subjects in accordance with the declaration of Helsinki before participation in the study. All subjects were recruited as part of the European project for sampling and biomarker optimization and harmonization in ALS and other motor neuron diseases (SOPHIA) at the Neuromuscular Disease Unit/ALS Clinic of the Cantonal Hospital St. Gallen (St. Gallen, Switzerland).

The patient sample consisted of 24 ALS patients (mean age = 62.6 years, standard deviation = 9.5 years, range = 48–84 years). According to the revised El Escorial criteria (Brooks et al. 2000), two had definite, ten had probable, seven probable laboratory-supported, and five possible ALS. Ten of these patients had bulbar-onset while 14 patients had limb-onset ALS. For the control group, 27 age-matched healthy subjects (mean age = 63.5 years, standard deviation = 8.4 years, range = 50–82 years) without prior history of neurological disorders were included.

2.2. Data acquisition

MR data acquisition was performed on a 3 T whole-body scanner (Achieva, Philips Healthcare, Best, the Netherlands, release 5.1.7), equipped with 80 mT/m gradients and an 8-element receive-only head coil array. For precise planning of the spectroscopic voxel, T_1-weighted images were recorded using a three-dimensional magnetization prepared rapid gradient-echo (MP-RAGE) sequence with the following parameters: repetition time (TR) = 8.2 ms, echo time (TE) = 3.8 ms, field of view = 240 × 240 x 160mm^3, voxel size = 1 × 1 × 1 mm^3, flip angle = 8°, scan duration = 6 min 35 s. Diffusion-weighted spectroscopic measurements of the PMC were obtained by incorporating bipolar diffusion gradients around the slice selective radiofrequency refocusing pulses within the standard point-resolved spectroscopic sequence (PRESS) with the following parameters: TR = 2000 ms, TE = 69 ms, voxel size = 15 × 30 × 25 mm^3, bandwidth = 2500 Hz, samples = 2048, number of signal averages (NSA) = 96, scan duration = 25 min 12 s. Diffusion weighting was applied along six non-collinear and non-coplanar directions with $\Delta b = 3000$ s/mm^2. Water suppression was achieved using an interleaved eight-pulse variable pulse power and optimized relaxation delays (VAPOR) pulse scheme (Tkac et al. 1999). In addition, an unsuppressed water spectrum with NSA = 8 was acquired for eddy current correction (Klose 1990). Implementation of the sequence was verified by in-vitro measurements in alcohol phantoms and the GE-MR spectroscopy “Braino” phantom and subsequent comparison of the results with literature values (Ellegood et al. 2011; Kan et al. 2012). For placement of the PRESS voxel, the central sulcus was first located in the most superior section of the transversal T_1-weighted images and then traced down. The voxel was thereafter centered on the precentral gyrus using the transversal images, with subsequent adjustment in the sagittal and coronal planes (Fig. 1). The voxel was positioned contralateral to the site of onset of clinical signs. When signs were symmetric (one limb-onset patient) or clinically absent in the limbs (nine bulbar-onset patients) and in the healthy controls, the voxel was placed in the motor cortex of the dominant hemisphere, as inferred by handedness. The shim volume was adjusted such that all metabolites of interest lay within its boundaries. In the ALS patients and a subgroup of ten healthy controls (mean age = 62.3 years, standard deviation = 5.6 years, range = 55–72 years, 5 female, 5 male), MR data acquisition was repeated three and six months after the baseline measurement. To replace the voxel as precisely as possible in subsequent measurements, the voxel position was saved at baseline in all three planes.

2.3. Clinical parameters

At each measurement time point, disease severity was assessed using the revised ALS functional rating scale (ALSFRS-R, maximum score = 48) with lower scores representing more disability (Cedarbaum et al. 1999). Finger dexterity was evaluated using the nine hole peg test (NHPT) (Kellor et al. 1971; Mathiowetz et al. 1985). For comparison, the NHPT was also performed in the control group.

2.4. Data processing

Data processing was performed using in-house software written in Matlab (The MathWorks, release 2017a, Natick, MA, USA). Optimization of the first and second order shims resulted in an in-vivo water line width of ≈4–8 Hz. Processing of the spectroscopic data included: eddy current correction, filtering with a 1 Hz exponential window, zero and first order (on the NAA peak) phase correction, frequency alignment, and averaging of the spectra. The resulting spectra were analyzed using TARQUIN (version 4.3.10) and “1H brain + Glth” as internal basis set (Wilson et al. 2011). The average signal-to-noise ratio (SNR) of NAA was 65.7 ± 11.3 (range = 41.2–94.1) in the non-diffusion-weighted and 38.9 ± 8.1 (range = 20.2–60.7) in the diffusion-weighted spectra. For diffusion analysis, the metabolite signals of tNAA, tCr, and tCho were used. The Cramér-Rao lower bounds of these metabolite were < 8% (mean = 1.4%, standard deviation = 0.88%, range = 0.3–7.3%). The diffusion tensor was calculated and the

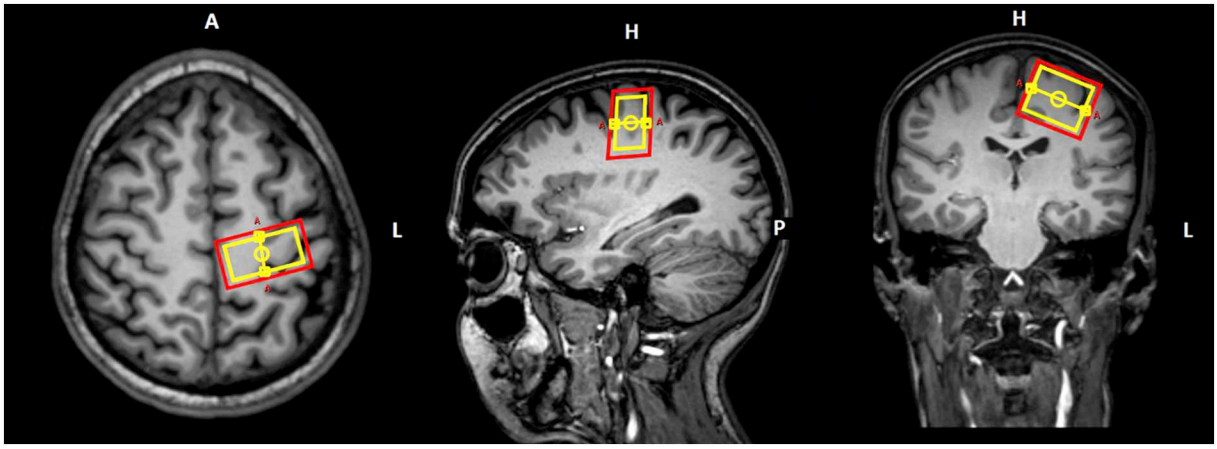

Fig. 1. Location of the PRESS voxel (yellow) and the corresponding shim (red) in the PMC superimposed onto the sagittal, coronal, and transversal T_1-weighted images.

eigenvalues were determined by diagonalization of the tensor to yield the mean diffusivity (MD), the axial diffusivity (AD), the radial diffusivity (RD), and the fractional anisotropy (FA) value. For comparison with previous work, tNAA/tCr, tNAA/tCho, and tCho/tCr ratios were determined from the non-diffusion-weighted spectra.

2.5. Statistical analysis

Statistical analysis of the data was performed in MATLAB (The MathWorks, release 2017a, Natick, MA, USA). Differences in age, in the diffusion parameters, and in the metabolite ratios between ALS patients and controls were assessed using two-sample *t*-tests. A Mann-Whitney *U* test was applied to determine whether there were differences in the NHPT durations between ALS patients and controls. The longitudinal changes in the diffusion parameters, metabolite ratios, and the ALSFRS-R scores of the ALS patients were analyzed using repeated measures ANOVA. Where Mauchly's test of sphericity indicated a violation of the assumption of sphericity, the Greenhouse-Geisser estimate was used. Changes in the NHPT durations over time were assessed using the Friedman test. CVs and ISVs were computed from the longitudinal data acquired in ten healthy controls. Finally, Spearman's rank correlations across times were calculated to delineate the relationship between the diffusion parameters/metabolite ratios and the clinical parameters (ALSFRS-R and NHPT).

For further exploratory statistical analysis, the patient group was subdivided into limb-onset (14 patients, mean age = 63.1 years, standard deviation = 9.8 years, range = 48–84 years) and bulbar-onset (10 patients, mean age = 61.9 years, standard deviation = 9.5 years, range = 48–74 years) ALS patients. One-way analysis of variance (ANOVA) followed by pairwise comparisons was used to assess difference in age, in the diffusion parameters, and in the metabolite ratios between patient groups and controls. A Kruskal-Wallis test followed by post-hoc comparisons was performed to evaluate differences in the NHPT durations between patient groups and controls. A two-sample t-test was performed to determine whether there were differences in the ALSFRS-R scores of limb-onset and bulbar-onset ALS patients.

Statistics was calculated on the log-transformed data where indicated and back transformation were performed where appropriate. A *p*-value of $p < .05$ was considered statistically significant. No corrections for multiple comparisons were performed and raw *p*-values are reported in this exploratory study since many of the parameters are expected to exhibit a high degree of correlation.

3. Results

Fig. 2 shows the non-diffusion-weighted and the diffusion-weighted spectra in two ALS patients with limb onset (Fig. 2A) and bulbar onset (Fig. 2B). The corresponding TARQUIN fits (red) are superimposed onto the raw data points (black). The location of the corresponding PRESS voxel in the PMC is depicted in the transversal plane of the T_1-weighted data. Fig. 3 shows representative non-diffusion-weighted and diffusion weighted spectra in one control subject.

3.1. Comparisons of patients versus controls at baseline

There was no significant difference in age between ALS patients and healthy controls ($p = .722$). The Mann-Whitney *U* test revealed that the median NHPT duration was significantly higher in ALS patients than in controls ($p < .001$). A summary of the clinical parameters of both groups is given in Table 1.

Table 2 summarizes the mean values and group comparisons of the diffusion parameters/metabolite ratios in patients versus controls. Statistical analysis showed that the MD values of all three metabolites were significantly higher in ALS patients than in controls. In addition, significant elevations were found in the AD and RD values of several metabolites. In contrast, no significant differences were found in the FA values.

3.2. Longitudinal analysis

Of the initial patients, eight patients were lost to follow up: one patient deceased after the baseline measurement, two patients could not further participate in the study after a rapid deterioration of their respiratory function and two patients after an acute deterioration in their general health condition. Finally, three patients had to be secondarily excluded due to insufficient data quality in subsequent measurements caused by excessive head motion. Thus, 16 ALS patients (mean age = 64.1 years, standard deviation = 10.0 years, range = 48–84 years, 8 male, 8 female) were included in the longitudinal analysis. Among these patients, four had bulbar-onset while 12 had limb-onset ALS. The NHPT durations (median and range) in the patient population were 24.5 s (17–75 s), 27.0 s (18–130 s), and 31.0 s (17–56 s) at baseline, three, and six months, respectively. The Friedman test indicated significant changes in the NHPT durations over time ($p = .030$). The ALSFRS-R scores (mean ± standard deviation) in the patient population were 39.0 ± 3.2 (range = 30–43), 37.6 ± 3.8 (range = 29–43), and 35.8 ± 4.2 (range = 27–42) at baseline, three, and six months, respectively. Repeated measures ANOVA showed a significant decline in the ALSFRS-R scores over time ($p < .001$). No significant changes in the diffusion parameters were observed but in line with previous work (Pohl et al. 2001), significant alterations in the tNAA/tCho ($p = .042$) and the tCho/tCr ($p = .048$) were found.

Table 3 summarizes the CVs and ISVs of the diffusion parameters/metabolite ratios assessed in ten healthy volunteers over a period of six

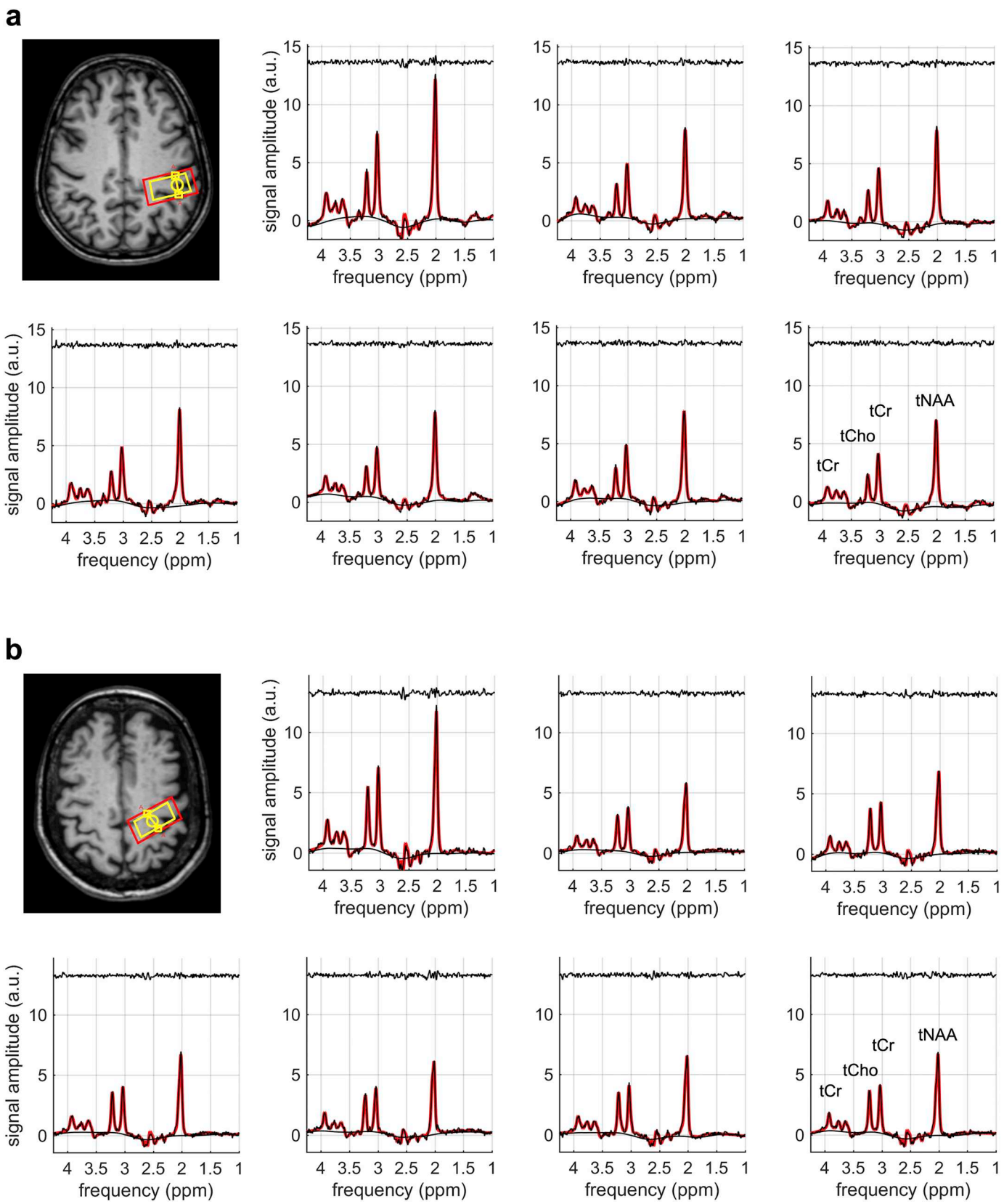

Fig. 2. Non-diffusion-weighted and diffusion-weighted spectra of (a) an ALS patient with limb onset (66 years, female) and (b) an ALS patient with bulbar onset (74 years, female). The TARQUIN fit (red) is superimposed onto the raw data points (black). The fit residuals are plotted above the spectra. The location of the PRESS voxel (yellow) and the corresponding shim (red) are depicted in the transversal plane of the T_1-weighted data.

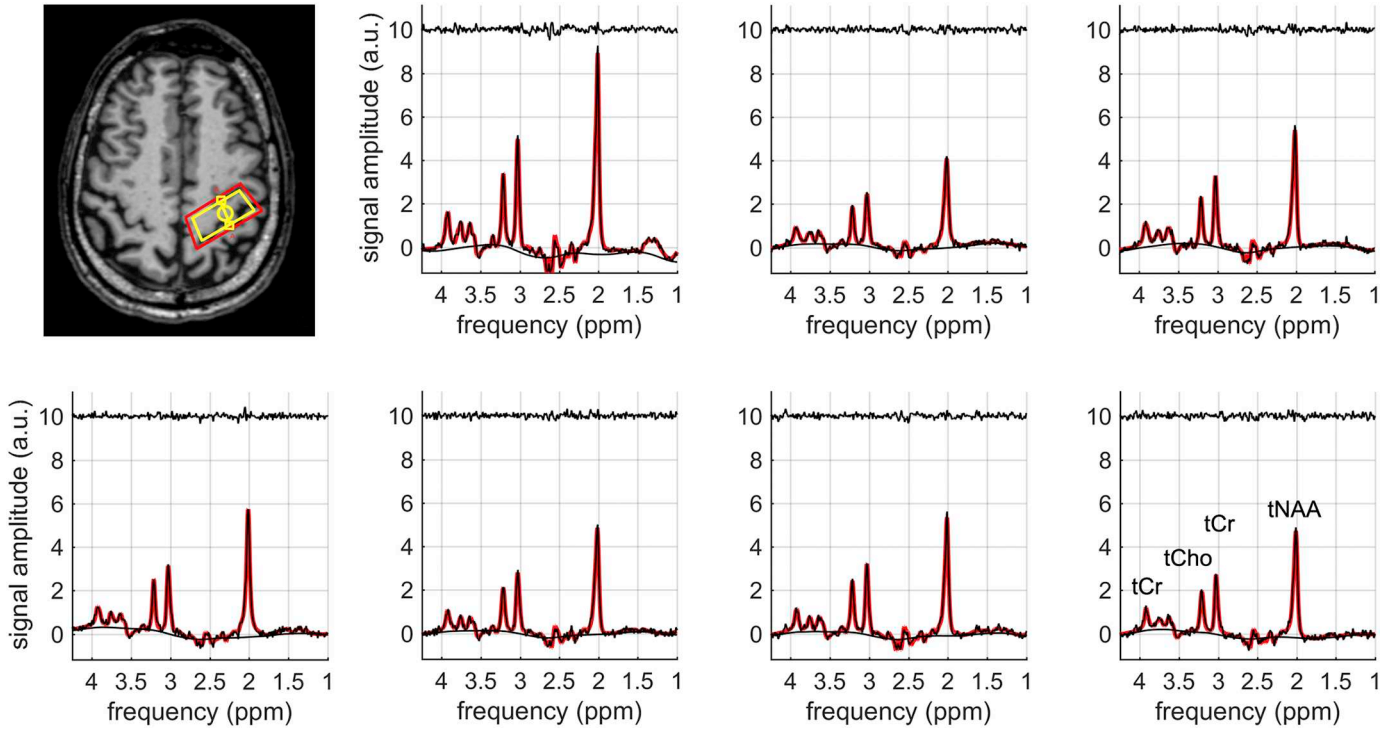

Fig. 3. Non-diffusion-weighted and diffusion-weighted spectra of a healthy control subject (56 years, male). The TARQUIN fit (red) is superimposed onto the raw data points (black). The fit residuals are plotted above the spectra. The location of the PRESS voxel (yellow) and the corresponding shim (red) are depicted in the transversal plane of the T_1-weighted data.

Table 1
Summary of the clinical parameters in the entire patient population and in the subgroups with limb-onset and bulbar-onset ALS as well as in the controls at baseline. Mean values and standard deviations are given unless indicated otherwise.

Parameter	ALS Patients	Limb-Onset ALS	Bulbar-Onset ALS	Controls
Female/male	13/11	8/6	5/5	13/14
Age (range) (years)	62.6 ± 9.5 (48–84)	63.1 ± 9.8 (48–84)	61.9 ± 9.5 (48–74)	63.5 ± 8.4 (50–82)
ALSFRS-R (range)	39.6 ± 3.0 (30–44)	39.5 ± 2.1 (36–43)	39.8 ± 4.0 (30–44)	–
NHPT (range) (s)[1]	24.0 (16–75)	31.8 (17–75)	25.0 (16–57)	19.3 (15–28)
Disease duration (months)	35.5 ± 29.9 (6–112)	48.2 ± 33.0 (9–112)	17.8 ± 11.0 (6–36)	–
Disease progression rate (1/months)[2]	0.4 ± 0.3 (0.1–1.1)	0.3 ± 0.3 (0.1–0.8)	0.6 ± 0.3 (0.2–1.1)	–

[1] Median values are given.
[2] Given as: (48-ALSFRS-R)/(months of disease duration).

months. The MD, AD, and RD values of the metabolites showed good to moderate precision while the FA values generally featured low precision.

3.3. Correlations with clinical parameters

No significant correlations of the diffusion parameters/metabolite ratios with the ALSFRS-R scores in the ALS patients across times were present. A weak correlation of the tNAA/tCr ratios with the durations of the NHPT was found ($\rho = -0.31$, $p = .016$) and a trend towards statistical significance was observed for the FA values of tCho ($p = .066$) and the RD values of tCr ($p = .070$).

3.4. Exploratory comparisons between limb-onset and bulbar-onset ALS patients and controls

There was no significant difference in age between the groups ($p = .894$). The Kruskal-Wallis test revealed that the mean ranks of NHPT durations were significantly different between groups ($p = .001$). Post-hoc analysis showed that there was a significant difference between the NHPT durations of limb-onset ALS patients and controls ($p < .001$). No significant differences between the NHPT durations of bulbar-onset ALS patients and controls ($p = .219$) and between both patients groups were observed ($p = .068$). There were no significant differences in the ALSFRS-R scores of limb-onset and bulbar-onset ALS patients ($p = .814$). A summary of the clinical parameters is given in Table 1.

Table 4 summarizes the mean values and group comparisons of the diffusion parameters/metabolite ratios at baseline. Microstructural alterations were more pronounced in the PMC of limb-onset ALS patients. In these patients, several diffusion parameters were significantly elevated relative to controls. It should be noted though that the MD of tNAA was significantly increased in bulbar-onset patients while there was only a trend towards statistical significance in limb-onset patients compared to controls. Beyond that, the tNAA/tCho ratios were significantly decreased in both patients groups while the tNAA/tCr ratios were significantly reduced in limb-onset ALS patients only relative to controls. Finally, no significant differences in the diffusion parameters/metabolite ratios were found between both patient groups.

4. Discussion

This is the first study to assess cell-specific microstructural alterations in the brain of ALS patients with DTS. Relative to DTI, DTS features improved pathologic specificity since microstructural alterations are evaluated by probing the diffusion of compartment-specific metabolites rather than water molecules, which reside in all tissue compartments. Increased values in the diffusivities of tNAA, tCr, and tCho

Table 2
Mean values and standard deviations of the diffusion parameters/metabolite ratios in patients and controls at baseline and *p*-values of the group comparisons. Statistically significant values are designated by an asterisk.

		Mean Values		Patients vs. Controls
Parameter		Patients	Controls	
MD ($\cdot 10^{-3}$ mm^2/s)	tNAA	0.186 ± 14.2%	0.168 ± 10.8%	0.006*
	tCr	0.189 ± 17.4%	0.170 ± 14.5%	0.016*
	tCho	0.168 ± 21.5%	0.137 ± 22.2%	0.002*
AD ($\cdot 10^{-3}$ mm^2/s)	tNAA	0.260 ± 20.8%	0.235 ± 14.2%	0.046*
	tCr	0.250 ± 22.8%	0.228 ± 16.0%	0.087
	tCho	0.241 ± 30.6%	0.197 ± 22.7%	0.011*
RD ($\cdot 10^{-3}$ mm^2/s)	tNAA	0.149 ± 11.4%	0.143 ± 13.5%	0.250
	tCr	0.158 ± 17.3%	0.140 ± 17.5%	0.015*
	tCho	0.125 ± 22.1%	0.104 ± 25.9%	0.011*
FA	tNAA	0.36 ± 35.1%	0.32 ± 32.7%	0.170
	tCr	0.32 ± 37.7%	0.32 ± 30.2%	0.978
	tCho	0.43 ± 40.1%	0.45 ± 27.9%	0.588
Ratios	tNAA/tCr	1.71 ± 9.2%	1.87 ± 8.7%	< 0.001*
	tNAA/tCho	7.24 ± 17.8%	8.55 ± 14.9%	< 0.001*
	tCho/tCr	0.24 ± 14.9%	0.22 ± 10.2%	0.045*

Table 3
Coefficients of variation and inter-subject variabilities of the diffusion parameters/metabolite ratios in the healthy controls as percentage.

Parameter		Coefficient of variation (%)	Inter-subject variability (%)
MD ($\cdot 10^{-3}$ mm^2/s)	tNAA	9.5	10.9
	tCr	9.0	7.1
	tCho	20.2	12.4
AD ($\cdot 10^{-3}$ mm^2/s)	tNAA	9.0	15.4
	tCr	7.7	9.9
	tCho	21.7	15.6
RD ($\cdot 10^{-3}$ mm^2/s)	tNAA	12.5	12.4
	tCr	16.3	7.1
	tCho	24.4	14.7
FA	tNAA	31.7	27.8
	tCr	40.1	21.4
	tCho	37.8	18.3
Ratios	tNAA/tCr	5.1	10.6
	tNAA/tCho	10.5	14.5
	tCho/tCr	11.0	9.2

were found in the PMC in ALS patients relative to controls. These findings suggest that microstructural alterations in the neuronal and glial compartments of the brain of ALS patients may be evaluated in vivo and non-invasively with DTS. Further analysis revealed that changes in tissue structure were more pronounced in ALS patients with limb onset than with bulbar onset relative to controls. This observation may be related to the fact that the PRESS voxel was positioned in the part of the PMC where the motor functions of the limbs are represented.

The metabolite ratios in the present work are in line with recent literature values (Verma et al. 2013). Furthermore, in agreement with previous spectroscopic studies, significantly reduced tNAA/tCr (Block et al. 1998; Chan et al. 1999; Pioro et al. 1994; Pohl et al. 2001; Wang et al. 2006) and tNAA/tCho (Block et al. 1998; Pohl et al. 2001; Wang et al. 2006) ratios have been observed in ALS patients compared to healthy controls. These findings have previously been interpreted as evidence of neuronal loss in ALS. However, reductions in tNAA may in part be a consequence of mitochondrial dysfunction in ALS (Bates et al. 1996). Moreover, in line with previous publications, significantly elevated tCho/tCr ratios (Block et al. 1998; Pohl et al. 2001) have been observed in ALS patients relative to healthy controls.

In keeping with neuronal loss and dysfunction, the present study revealed significantly increased values in the diffusivity of tNAA in ALS patients relative to controls. In patients with neuropsychiatric systemic lupus erythematosus symptoms (NPLSE) such changes have been attributed to neuronal damage (Ercan et al. 2016). Alternatively, mitochondrial dysfunction, as observed in ALS, has been hypothesized to result in increased values in diffusivity of tNAA (Du et al. 2013). In contrast to the present results, significantly reduced values in the

Table 4
Mean values and standard deviations of the diffusion parameters/metabolite ratios of limb-onset and bulbar-onset ALS patients at baseline and p-values of the post-hoc comparisons of the one-way ANOVA. Statistically significant values are designated by an asterisk.

		Mean Values of ALS Patients		Statistical Comparisons		
Parameter		Limb Onset	Bulbar Onset	Limb Onset vs. Controls	Bulbar Onset vs. Controls	Limb vs. Bulbar Onset
MD ($\cdot 10^{-3}$ mm^2/s)	tNAA	0.182 ± 13.6%	0.187 ± 14.1%	0.088	0.040*	0.861
	tCr	0.198 ± 19.9%	0.183 ± 14.8%	0.019*	0.511	0.435
	tCho	0.173 ± 23.3%	0.160 ± 18.0%	0.007*	0.181	0.666
AD ($\cdot 10^{-3}$ mm^2/s)	tNAA	0.263 ± 21.7%	0.257 ± 20.5%	0.152	0.380	0.949
	tCr	0.260 ± 23.5%	0.237 ± 21.8%	0.101	0.832	0.488
	tCho	0.252 ± 30.1%	0.224 ± 31.7%	0.019*	0.423	0.542
RD ($\cdot 10^{-3}$ mm^2/s)	tNAA	0.148 ± 12.3%	0.149 ± 10.5%	0.644	0.595	0.986
	tCr	0.164 ± 17.8%	0.154 ± 17.4%	0.029*	0.404	0.612
	tCho	0.127 ± 24.0%	0.123 ± 19.5%	0.044*	0.217	0.920
FA	tNAA	0.37 ± 35.8%	0.35 ± 35.9%	0.378	0.683	0.944
	tCr	0.33 ± 26.3%	0.31 ± 52.5%	0.973	0.943	0.886
	tCho	0.47 ± 33.3%	0.37 ± 51.4%	0.967	0.361	0.326
Ratios	tNAA/tCr	1.68 ± 8.7%	1.74 ± 10.0%	0.033*	0.084	0.667
	tNAA/tCho	7.19 ± 19.0%	7.31 ± 16.9%	0.007*	0.033*	0.974
	tCho/tCr	0.23 ± 15.1%	0.24 ± 15.5%	0.250	0.215	0.969

diffusivity of tNAA have been found in normal-appearing white matter of patients with multiple sclerosis (MS) relative to healthy controls. The different behaviors in diffusivity of tNAA in ALS and MS patients may reflect different pathological mechanisms associated with these diseases (e.g. primarily axonal damage in MS versus primarily neuronal damage and secondary axonal degeneration in ALS (Fogarty et al. 2016)).

In agreement with the present work, increased diffusivities of tCr and tCho have been observed in patients with NPLSE compared to healthy controls. These elevations were interpreted as reflecting both astrocytic and microglial reactivity in response to inflammation and/or ischaemia. According to the authors, reactivity-related cellular hypertrophy and thickening of the processes near the soma would thereby result in an increase of the intracellular space, and a simultaneous decrease in molecular crowding and intracellular tortuosity leading to increased diffusivity in the cytosol. A similar mechanism may occur in ALS patients since inflammatory processes and immune reactivity are assumed to play a role in the pathogenesis of ALS (Philips and Robberecht 2011) and both reactive microglia (Kawamata et al. 1992; Turner et al. 2004) and astrocytes (Kamo et al. 1987; Murayama et al. 1991; Nagy et al. 1994) have been found in the PMC surrounding degenerating neurons. Beyond that, the results of a recent study indicate a mechanistic link between tissue integrity and glial activation in patients with sporadic ALS (Alshikho et al. 2016). Decreased FA values of water were thereby co-localized with increased uptake of a glial marker. In contrast to the aforementioned study, the results of the present work establish a more direct link since structural changes in glial cells were explored by probing the diffusion of two predominantly glial metabolites instead of water, which is present in all tissue types.

In line with a previous study (Pohl et al. 2001), longitudinal analysis revealed significant changes in the tNAA/tCho and tCho/tCr ratios over time. However, no alterations in the diffusion parameters were observed. The relatively short follow-up period in the present study is likely insufficient to capture the evolution of the diffusion parameters over the course of the disease and in addition faster progressing patients were lost to follow up. Since a wide range of survival times is observed in ALS ranging from a few months to several decades (Beghi et al. 2006), it is difficult to determine the optimum follow-up period and larger patient cohorts are required to reliably evaluate longitudinal changes in the diffusion parameters.

The diffusion parameters in the present work are similar to those observed in another DTS study (Ellegood et al. 2011). With the exception of the FA values, the diffusion parameters showed good to moderate precision. The limited precision of the FA values may be the reason why no significant differences were observed in the group analysis. Precision of the parameter estimates may be increased by transition to higher field strengths not only due to the associated increase in SNR but also because of improved spectral separation, which allows for a more reliable estimation of the metabolite signals. Alternatively, higher field strengths would permit reducing partial volume effects by decreasing the size of the PRESS voxel.

No significant correlations of the parameters with disease severity, as assessed by the ALSFRS-R score, were detected. The lack of correlation may be due to the relatively low number of patients and the limited range of ALSFRS-R scores in the patient sample. Beyond that, functional scales are far more sensitive to lower motor neuron involvement and the associated muscle wasting rather than to upper motor neuron injury. Nevertheless, some studies have found significant correlations for instance of the ALSFRS-R scores with the tNAA/Cr ratios (Wang et al. 2006). There was a significant albeit weak correlation of the NHPT durations with the tNAA/tCr ratios. Likely due to the limited number of study participants, no significant correlations of the NHPT with the diffusion parameters was found.

Differences were observed for both limb-onset and bulbar-onset patients relative to controls but microstructural alterations were more pronounced in the PMC of limb-onset patients. This finding may be related to the fact that the PRESS voxel was positioned in the part of the PMC where the motor functions of the limbs are represented.

The main limitation of the present work is the relatively small patient population and the short follow-up period in this exploratory study. Furthermore, due to the relatively long scan duration microstructural alterations were only investigated in the PMC of ALS patients. Future studies which include larger patient cohorts and explore additional brain structures, are necessary to confirm the preliminary results of the present work and in particular to permit comprehensive evaluation of differences between onset types. The results of the present work indicate that acquisition of three diffusion directions and subsequent computation of the apparent diffusion coefficient may suffice for evaluation of cell-specific microstructural alterations. In this manner, scan time may be decreased and additional brain structures could be explored. Alternatively, if data were acquired at higher field strength fewer NSA would be necessary due to the intrinsically higher SNR. Furthermore, recent technical developments permit assessing the diffusion properties of brain metabolites beyond tNAA, tCr, and tCho (Landheer et al. 2017), which may aid the evaluation of pathogenesis in ALS. In particular, myoinositol is of interest as a counterpart to tNAA since it represents the complementary major intracellular compartment in the central nervous system (Palombo et al. 2017).

In conclusion, the results of the present study show for the first time that DTS permits measuring cell-type specific microstructural alterations in ALS patients in vivo and non-invasively by probing the diffusion of intracellular brain metabolites, which are reflective of the neuronal and glial compartments. Incorporated into a comprehensive scan protocol with other existing microstructural MR imaging methods such as DTI or susceptibility-weighted imaging, the technique may help unravel the pathogenic mechanisms that underlie neurodegeneration in ALS.

Acknowledgments

This is an EU Joint Programme Neurodegenerative Disease Research (JPND) project. The project is supported through the following funding organizations under the aegis of JPND www.jpnd.eu: France, Agence Nationale de la Recherche; Germany, Bundesministerium für Bildung und Forschung; Ireland, Health Research Board; Italy, Ministero della Salute; The Netherlands, The Netherlands Organisation for Health Research and Development; Poland, Narodowe Centrum Badan i Rozwoju; Portugal, Fundação a Ciência e a Tecnologia; Spain, Ministerio de Ciencia e Innovación; Switzerland, Schweizerischer Nationalfonds zur Förderung der wissenschaftlichen Forschung; Turkey, Tübitak; United Kingdom, Medical Research Council. SNF Grant 31ND30_141622.

Declaration of interest

The authors declare that they have no competing interest.

References

Alshikho, M.J., Zurcher, N.R., Loggia, M.L., Cernasov, P., Chonde, D.B., Izquierdo Garcia, D., Yasek, J.E., Akeju, O., Catana, C., Rosen, B.R., Cudkowicz, M.E., Hooker, J.M., Atassi, N., 2016. Glial activation colocalizes with structural abnormalities in amyotrophic lateral sclerosis. Neurology 87, 2554–2561.

Basser, P.J., Mattiello, J., Lebihan, D., 1994a. Estimation of the effective self-diffusion tensor from the NMR spin echo. J. Magn. Reson. B 103, 247–254.

Basser, P.J., Mattiello, J., Lebihan, D., 1994b. MR diffusion tensor spectroscopy and imaging. Biophys. J. 66, 259–267.

Bates, T.E., Strangward, M., Keelan, J., Davey, G.P., Munro, P.M., Clark, J.B., 1996. Inhibition of N-acetylaspartate production: implications for 1H MRS studies in vivo. Neuroreport 7, 1397–1400.

Beghi, E., Logroscino, G., Chio, A., Hardiman, O., Mitchell, D., Swingler, R., Traynor, B.J., Consortium, E., 2006. The epidemiology of ALS and the role of population-based registries. Biochim. Biophys. Acta 1762, 1150–1157.

Block, W., Karitzky, J., Traber, F., Pohl, C., Keller, E., Mundegar, R.R., Lamerichs, R., Rink, H., Ries, F., Schild, H.H., Jerusalem, F., 1998. Proton magnetic resonance

spectroscopy of the primary motor cortex in patients with motor neuron disease: subgroup analysis and follow-up measurements. Arch. Neurol. 55, 931–936.
Bodini, B., Branzoli, F., Poirion, E., Garcia-Lorenzo, D., Didier, M., Maillart, E., Socha, J., Bera, G., Lubetzki, C., Ronen, I., Lehericy, S., Stankoff, B., 2018. Dysregulation of energy metabolism in multiple sclerosis measured in vivo with diffusion-weighted spectroscopy. Mult. Scler. 24, 313–321.
Bowen, B.C., Pattany, P.M., Bradley, W.G., Murdoch, J.B., Rotta, F., Younis, A.A., Duncan, R.C., Quencer, R.M., 2000. MR imaging and localized proton spectroscopy of the precentral gyrus in amyotrophic lateral sclerosis. AJNR Am. J. Neuroradiol. 21, 647–658.
Bradley, W.G., Bowen, B.C., Pattany, P.M., Rotta, F., 1999. 1H-magnetic resonance spectroscopy in amyotrophic lateral sclerosis. J. Neurol. Sci. 169, 84–86.
Brand, A., Richter-Landsberg, C., Leibfritz, D., 1993. Multinuclear NMR studies on the energy metabolism of glial and neuronal cells. Dev. Neurosci. 15, 289–298.
Brooks, B.R., Miller, R.G., Swash, M., Munsat, T.L., 2000. El Escorial revisited: revised criteria for the diagnosis of amyotrophic lateral sclerosis. Amyotroph. Lateral Scler. Other Motor Neuron. Disord. 1, 293–299.
Cedarbaum, J.M., Stambler, N., Malta, E., Fuller, C., Hilt, D., Thurmond, B., Nakanishi, A., 1999. The ALSFRS-R: a revised ALS functional rating scale that incorporates assessments of respiratory function. BDNF ALS Study Group (Phase III). J. Neurol. Sci. 169, 13–21.
Chan, S., Shungu, D.C., Douglas-Akinwande, A., Lange, D.J., Rowland, L.P., 1999. Motor neuron diseases: comparison of single-voxel proton MR spectroscopy of the motor cortex with MR imaging of the brain. Radiology 212, 763–769.
Colvin, D.C., Yankeelov, T.E., Does, M.D., Yue, Z., Quarles, C., Gore, J.C., 2008. New insights into tumor microstructure using temporal diffusion spectroscopy. Cancer Res. 68, 5941–5947.
Du, F., Cooper, A.J., Thida, T., Shinn, A.K., Cohen, B.M., Ongur, D., 2013. Myelin and axon abnormalities in schizophrenia measured with magnetic resonance imaging techniques. Biol. Psychiatry 74, 451–457.
Ellegood, J., Hanstock, C.C., Beaulieu, C., 2006. Diffusion tensor spectroscopy (DTS) of human brain. Magn. Reson. Med. 55, 1–8.
Ellegood, J., Hanstock, C.C., Beaulieu, C., 2011. Considerations for measuring the fractional anisotropy of metabolites with diffusion tensor spectroscopy. NMR Biomed. 24, 270–280.
Ercan, E., Magro-Checa, C., Valabregue, R., Branzoli, F., Wood, E.T., Steup-Beekman, G.M., Webb, A.G., Huizinga, T.W., van Buchem, M.A., Ronen, I., 2016. Glial and axonal changes in systemic lupus erythematosus measured with diffusion of intracellular metabolites. Brain 139, 1447–1457.
Fogarty, M.J., Mu, E.W., Noakes, P.G., Lavidis, N.A., Bellingham, M.C., 2016. Marked changes in dendritic structure and spine density precede significant neuronal death in vulnerable cortical pyramidal neuron populations in the SOD1(G93A) mouse model of amyotrophic lateral sclerosis. Acta Neuropathol. Commun. 4, 77.
Gredal, O., Rosenbaum, S., Topp, S., Karlsborg, M., Strange, P., Werdelin, L., 1997. Quantification of brain metabolites in amyotrophic lateral sclerosis by localized proton magnetic resonance spectroscopy. Neurology 48, 878–881.
Harada, M., Uno, M., Hong, F., Hisaoka, S., Nishitani, H., Matsuda, T., 2002. Diffusion-weighted in vivo localized proton MR spectroscopy of human cerebral ischemia and tumor. NMR Biomed. 15, 69–74.
Kamo, H., Haebara, H., Akiguchi, I., Kameyama, M., Kimura, H., Mcgeer, P.L., 1987. A distinctive distribution of reactive astroglia in the precentral cortex in amyotrophic-lateral-sclerosis. Acta Neuropathol. 74, 33–38.
Kan, H.E., Techawiboonwong, A., van Osch, M.J., Versluis, M.J., Deelchand, D.K., Henry, P.G., Marjanska, M., van Buchem, M.A., Webb, A.G., Ronen, I., 2012. Differences in apparent diffusion coefficients of brain metabolites between grey and white matter in the human brain measured at 7 T. Magn. Reson. Med. 67, 1203–1209.
Kawamata, T., Akiyama, H., Yamada, T., McGeer, P.L., 1992. Immunologic reactions in amyotrophic lateral sclerosis brain and spinal cord tissue. Am. J. Pathol. 140, 691–707.
Kellor, M., Frost, J., Silberberg, N., Iversen, I., Cummings, R., 1971. Hand strength and dexterity. Am. J. Occup. Ther. 25, 77–83.
Klose, U., 1990. In vivo proton spectroscopy in presence of eddy currents. Magn. Reson. Med. 14, 26–30.
Landheer, K., Schulte, R., Geraghty, B., Hanstock, C., Chen, A.P., Cunningham, C.H., Graham, S.J., 2017. Diffusion-weighted J-resolved spectroscopy. Magn. Reson. Med. 78, 1235–1245.
Le Belle, J.E., Harris, N.G., Williams, S.R., Bhakoo, K.K., 2002. A comparison of cell and tissue extraction techniques using high-resolution 1H-NMR spectroscopy. NMR Biomed. 15, 37–44.
Liu, Z., Zheng, D., Wang, X., Zhang, J., Xie, S., Xiao, J., Jiang, X., 2011. Apparent diffusion coefficients of metabolites in patients with MELAS using diffusion-weighted MR spectroscopy. AJNR Am. J. Neuroradiol. 32, 898–902.
Mathiowetz, V., Weber, K., Kashman, N., Volland, G., 1985. Adult norms for the nine hole peg test of finger dexterity. Occup. Ther. J. Res. 5, 24–38.
Merboldt, K.D., Horstermann, D., Hanicke, W., Bruhn, H., Frahm, J., 1993. Molecular self-diffusion of intracellular metabolites in rat brain in vivo investigated by localized proton NMR diffusion spectroscopy. Magn. Reson. Med. 29, 125–129.
Murayama, S., Inoue, K., Kawakami, H., Bouldin, T.W., Suzuki, K., 1991. A unique pattern of astrocytosis in the primary motor area in amyotrophic lateral sclerosis. Acta Neuropathol. 82, 456–461.
Nagy, D., Kato, T., Kushner, P.D., 1994. Reactive astrocytes are widespread in the cortical gray-matter of amyotrophic-lateral-sclerosis. J. Neurosci. Res. 38, 336–347.
Nicolay, K., van der Toorn, A., Dijkhuizen, R.M., 1995. In vivo diffusion spectroscopy. An overview. NMR Biomed. 8, 365–374.
Palombo, M., Shemesh, N., Ronen, I., Valette, J., 2017. Insights into brain microstructure from in vivo DW-MRS. NeuroImage. https://doi.org/10.1016/j.neuroimage.2017.11.028. (Nov 16, pii: S1053-8119(17)30942-4, Epub ahead of print).
Philips, T., Robberecht, W., 2011. Neuroinflammation in amyotrophic lateral sclerosis: role of glial activation in motor neuron disease. Lancet Neurol. 10, 253–263.
Pioro, E.P., Antel, J.P., Cashman, N.R., Arnold, D.L., 1994. Detection of cortical neuron loss in motor neuron disease by proton magnetic resonance spectroscopic imaging in vivo. Neurology 44, 1933–1938.
Pohl, C., Block, W., Karitzky, J., Traber, F., Schmidt, S., Grothe, C., Lamerichs, R., Schild, H., Klockgether, T., 2001. Proton magnetic resonance spectroscopy of the motor cortex in 70 patients with amyotrophic lateral sclerosis. Arch. Neurol. 58, 729–735.
Posse, S., Cuenod, C.A., Le Bihan, D., 1993. Human brain: proton diffusion MR spectroscopy. Radiology 188, 719–725.
Rooney, W.D., Miller, R.G., Gelinas, D., Schuff, N., Maudsley, A.A., Weiner, M.W., 1998. Decreased N-acetylaspartate in motor cortex and corticospinal tract in ALS. Neurology 50, 1800–1805.
Rowland, L.P., Shneider, N.A., 2001. Amyotrophic lateral sclerosis. N. Engl. J. Med. 344, 1688–1700.
Schuff, N., Rooney, W.D., Miller, R., Gelinas, D.F., Amend, D.L., Maudsley, A.A., Weiner, M.W., 2001. Reanalysis of multislice (1)H MRSI in amyotrophic lateral sclerosis. Magn. Reson. Med. 45, 513–516.
Simmons, M.L., Frondoza, C.G., Coyle, J.T., 1991. Immunocytochemical localization of N-acetyl-aspartate with monoclonal antibodies. Neuroscience 45, 37–45.
Suhy, J., Miller, R.G., Rule, R., Schuff, N., Licht, J., Dronsky, V., Gelinas, D., Maudsley, A.A., Weiner, M.W., 2002. Early detection and longitudinal changes in amyotrophic lateral sclerosis by (1)H MRSI. Neurology 58, 773–779.
Tkac, I., Starcuk, Z., Choi, I.Y., Gruetter, R., 1999. In vivo 1H NMR spectroscopy of rat brain at 1 ms echo time. Magn. Reson. Med. 41, 649–656.
Turner, M.R., Cagnin, A., Turkheimer, F.E., Miller, C.C., Shaw, C.E., Brooks, D.J., Leigh, P.N., Banati, R.B., 2004. Evidence of widespread cerebral microglial activation in amyotrophic lateral sclerosis: an [11C](R)-PK11195 positron emission tomography study. Neurobiol. Dis. 15, 601–609.
Urenjak, J., Williams, S.R., Gadian, D.G., Noble, M., 1993. Proton nuclear magnetic resonance spectroscopy unambiguously identifies different neural cell types. J. Neurosci. 13, 981–989.
Van Zijl, P.C., Moonen, C.T., Faustino, P., Pekar, J., Kaplan, O., Cohen, J.S., 1991. Complete separation of intracellular and extracellular information in NMR spectra of perfused cells by diffusion-weighted spectroscopy. Proc. Natl. Acad. Sci. U. S. A. 88, 3228–3232.
Verma, G., Woo, J.H., Chawla, S., Wang, S., Sheriff, S., Elman, L.B., McCluskey, L.F., Grossman, M., Melhem, E.R., Maudsley, A.A., Poptani, H., 2013. Whole-brain analysis of amyotrophic lateral sclerosis by using echo-planar spectroscopic imaging. Radiology 267, 851–857.
Wang, S., Poptani, H., Woo, J.H., Desiderio, L.M., Elman, L.B., McCluskey, L.F., Krejza, J., Melhem, E.R., 2006. Amyotrophic lateral sclerosis: diffusion-tensor and chemical shift MR imaging at 3.0 T. Radiology 239, 831–838.
Wilson, M., Reynolds, G., Kauppinen, R.A., Arvanitis, T.N., Peet, A.C., 2011. A constrained least-squares approach to the automated quantitation of in vivo 1H magnetic resonance spectroscopy data. Magn. Reson. Med. 65, 1–12.
Wood, E.T., Ronen, I., Techawiboonwong, A., Jones, C.K., Barker, P.B., Calabresi, P., Harrison, D., Reich, D.S., 2012. Investigating axonal damage in multiple sclerosis by diffusion tensor spectroscopy. J. Neurosci. 32, 6665–6669.
Zheng, D.D., Liu, Z.H., Fang, J., Wang, X.Y., Zhang, J., 2012. The effect of age and cerebral ischemia on diffusion-weighted proton MR spectroscopy of the human brain. AJNR Am. J. Neuroradiol. 33, 563–568.
Zielman, R., Wijnen, J.P., Webb, A., Onderwater, G.L.J., Ronen, I., Ferrari, M.D., Kan, H.E., Terwindt, G.M., Kruit, M.C., 2017. Cortical glutamate in migraine. Brain 140, 1859–1871.